Functional analysis of *HOXA10* and *HOXB4* in human medulloblastoma cell lines

RICARDO BONFIM-SILVA[1], FERNANDA URSOLI FERREIRA MELO[2], CAROLINA HASSIBE THOMÉ[3], KURUVILLA JOSEPH ABRAHAM[4], FÁBIO AUGUSTO LABRE DE SOUZA[1], FERNANDO SILVA RAMALHO[5], HÉLIO RUBENS MACHADO[6], RICARDO SANTOS DE OLIVEIRA[6], ANGELO A. CARDOSO[8], DIMAS TADEU COVAS[7] and APARECIDA MARIA FONTES[1]

[1]Department of Genetics, [2]Regional Blood Center of Ribeirão Preto, Departments of [3]Biochemistry and Immunology, [4]Pediatrics, [5]Pathology and Legal Medicine, Ribeirão Preto Medical School, [6]Division of Pediatric Neurosurgery of the Department of Surgery and Anatomy, University Hospital of Ribeirão Preto Medical School, [7]Department of Internal Medicine, University of São Paulo, Av. Bandeirantes, 3900, Monte Alegre 14049-900, Ribeirão Preto, São Paulo, Brazil; [8]Center for Gene Therapy, City of Hope Alpha Stem Cell Clinic, Duarte, CA 91010, USA

Received July 16, 2017; Accepted September 28, 2017

DOI: 10.3892/ijo.2017.4151

Abstract. Medulloblastoma (MB) is a malignant childhood brain tumor which at molecular level is classified into at least four major subtypes: WNT, SHH, group C and group D differing in response to treatment. Previous studies have associated changes in expression levels and activation of certain *HOX* genes with MB development. In the present study, we investigate the role of *HOX* genes in two attributes acquired by tumor cells: migration and proliferation potential, as well as, *in vivo* tumorigenic potential. We analyzed UW402, UW473, DAOY and ONS-76 human pediatric MB cell lines and cerebellum primary cultures. Two-color microarray-based gene expression analysis was used to identify differentially expressed *HOX* genes. Among the various *HOX* genes significantly overexpressed in DAOY and ONS-76 cell lines compared to UW402 and UW473 cell lines, *HOXA10* and *HOXB4* were selected for further analysis. The expression levels of these *HOX* genes were validated by real-time PCR. A mouse model was used to study the effect of the *HOXA10* and *HOXB4* genes on the *in vivo* tumorigenic potential and the *in vitro* proliferative and migration potential of MB cell lines. Our results show that the inhibition of *HOXA10* in DAOY cell line led to increased *in vitro* cell migration while *in vitro* cell proliferation or *in vivo* tumorigenic potential were unaffected. We also observed that induced expression of *HOXB4* in the UW473 cell line significantly reduced *in vitro* cell proliferation and migration capability of UW473 cells with no effect on the *in vivo* tumorigenicity. This suggests that *HOXA10* plays a role in migration events and the *HOXB4* gene is involved in proliferation and migration processes of medulloblastoma cells, however, it appears that these genes are not essential for the tumorigenic process of these cells.

Correspondence to: Professor Aparecida Maria Fontes, Department of Genetics, Ribeirão Preto Medical School, University of São Paulo, Av. Bandeirantes, 3900, Monte Alegre 14049-900, Ribeirão Preto, São Paulo, Brazil
E-mail: aparecidamfontes@usp.br; aparecidamfontes@gmail.com

Key words: medulloblastoma, *HOXA10*, *HOXB4*, microarray, migration potential, proliferative potential

Introduction

Medulloblastoma (MB) represents a genetically and epigenetically heterogeneous group of neuroepithelial primary tumors arising from the cerebellum (1). The World Health Organization (WHO) has classified four histological variants of MB which include classic, desmoplastic nodular (MB/N), MB with extensive nodularity (MBEN) and large cell/anaplastic type (LC/A) (2). Later, Garré *et al* proposed the classification of MB into two groups, standard-risk (SR) and high-risk (HR) groups (3,4) according to the risk-adapted treatments. In 2012, an international collaborative microarray study established four molecular subgroups in MB (WNT, SHH, group 3 and 4) (5,6). It is noteworthy that Gibson *et al* (7) found that WNT- and SHH-subtype medulloblastoma have different anatomical locations. For example, the WNT-Subtype is located within the IV ventricle and arises at the dorsal surface of the brainstem, while the SHH-subtype arises within the cerebellar hemispheres. Current treatment protocols are dependent on the age of patients; for patients older than 36 months of age options include maximal safe tumor resection followed by craniospinal radiotherapy and chemotherapy. Infants younger than 36 months do not receive radiotherapy due the risk of severe side-effects (8). Cure rates are dependent on the MB molecular subtype. Patients with MB-WNT have a cure rate of over 90%, while in patients with MB-group 3 40-60% face chemo or radio-resistance or relapse (8,9). This variation in treatment response is a motivation to better understand the biology of these tumors, including gene expression patterns, in

order to increase cure rates and/or to reduce treatment-related sequelae.

An earlier comprehensive sequence analysis study in 88 pediatric MB samples led to the discovery of a gene, histone-lysine N-methyltransferase *MLL2*, not previously known to be altered in MBs (10). In 14% of MB patients in the same study somatic mutations were observed in *MLL2*, which is known to be a member of the trithorax complex that induces epigenetic marks that correlate with accessible euchromatin (11). The connection between MLL2 alterations and tumorigenesis has not been investigated in medulloblastoma. One possibility is that, the *MLL2* gene (new approved symbol KMT2D), which codifies the MLL2 protein and which plays a role in maintaining *HOX* gene expression (10,12) might deregulate *HOX* gene expression in cancer. *HOX* genes encode evolutionarily conserved homeodomain-containing transcription factors and in humans there are four clusters named *HOXA*, *HOXB*, *HOXC* and *HOXD*, which are located on chromosomes 7p14, 17a21, 12q13 and 2q31, respectively.

An additional motivation for studying HOX gene expression in MB arises from the role of HOX genes in cerebellum development. As described in Wang and Zoghbi (13), cerebellum development commences from the dorsal region of the posterior neural tube. Two of the regions of the posterior neural tube, the mesencephalon and the metencephalon depend on molecular signals received from the Isthmus Organizer (IO). The *Otx-2* (MB oncogene) plays a role in IO development while various genes in *HOX* family affect metencephalon development (13).

Moreover, the expression of *HOX* genes is not limited to the embryonic phase of development (14). Takahashi *et al* (15) studied the expression profiles of 39 HOX genes in 20 different human adult normal organs by real-time PCR. They showed that in the cerebellum six HOX genes are expressed, among them: HOXB2, HOXB3, HOXB4, HOXC4, HOXD1 and HOXD3. Other studies have investigated the expression of HOX genes in cerebellum suggesting that the number of HOX genes transcribed in the cerebellum can be even higher. For example, recently, Hutlet *et al* (16) demonstrated low expression of 21 specific HOX genes in adult mice cerebella, all belonging to paralogy groups (PG) 1-8 (16). These data suggest complex patterns of HOX expression in the cerebellum, which in turn suggest the relevance of multiple HOX gene regulation mechanisms. These mechanisms include the use of multiple promoters, alternative splicing, antisense transcripts, long non-coding RNA, miRNA, as well as some translation controls (16,17).

In some cancers, certain *HOX* genes may function as oncogene or tumor suppressor genes (18). For example, in prostate, breast and colorectal cancers loss-of-function of *HOXB13* mutations suggests that *HOXB13* may function as a tumor suppressor gene (19). On the other hand, in breast and colorectal cancer, upregulation of *HOXB7* promotes cell proliferation, which implies that it might function as an oncogene (20,21). Apart from loss of function, additional progress has been made in understanding changes in expression levels and the activation of certain *HOX* genes and cancer development (22,23). In brain tumors, the deregulation of *HOX* genes has been described in glioblastoma (24-27) neuroblastoma (28,29), tumor atypical teratoid rhabdoid, juvenile pilocytic astrocytoma and ependymomas (30). In medulloblastoma, Bodey *et al* (31) observed by immunocytochemistry techniques that *HOXB3*, *HOXB4* and *HOXC6* proteins were expressed in medulloblastoma tissues. In 2014, Chakravadhanula *et al* (30) reported that *HOXC4-6*, *HOXC8-13*, *HOXD3-4*, *HOXD8-11* and *HOXD13* genes were upregulated and *HOXD1* gene was downregulated in medulloblastoma tissues when compared to control tissues.

Recently, in order to elucidate epigenetic changes that contribute to medulloblastoma progression, Vo *et al* (32) demonstrated through the use of engineered deletions of *Ezh2* by gene editing nucleases, that inactivation of *Ezh2* drives aggressive medulloblastoma. *Ezh2* is a member of the polycomb complex known to induce marks that correlate with heterochromatinization and mediate repression of *HOX* genes (33). In addition to repression, the authors showed that loss of *Ezh2* is also accompanied by upregulation of several *HOX* genes (32).

These studies suggest that several epigenetic mechanisms of *HOX* regulation might play a role in medulloblastoma. However, the role of *HOX* gene dysregulation in medulloblastoma has not been investigated. In 2011, a seminal study (34) suggested ten attributes which are acquired by tumor cells and which also sustain the malignant behavior in various types of cancer. In this study, we investigate the role of two specific *HOX* genes, *HOXA10* and *HOXB4*, in two of these attributes in meduloblastoma: migration and proliferation potential.

Materials and methods

Cell lines. Four independent medulloblastoma cell lines (UW402, UW473, DAOY and ONS-76) were used in this study. UW402 and UW473 cell lines, have been previously characterized regarding chromosomal heterogeneity, instability profiles, cell morphology, cell population doubling time, colony-forming efficiency as well as chemo-sensitivity heterogeneity (35). Both DAOY and ONS-76 cell lines are long-established MB cell lines (36-38). The ONS-76, UW402 and UW473 cell lines were kindly provided by the Laboratory of Pediatric Oncology of the Clinical Hospital of the Medical School of Ribeirão Preto (CHMSRP), while the DAOY cell line was purchased from the American Type Culture Collection (ATCC: HTB-186; ATTC, Manassas, VA, USA).

The three cerebellum primary cultures (CP4, CP5 and CP6) were generated from cerebellum specimens that were harvested from infants at autopsy in the Pathology Service of the CHMSRP. CP4 was obtained from cerebellum of a full term newborn who died at two months old. CP5 and CP6 were collected from the cerebella of two infants born at 22 and 23 weeks of gestation, respectively, who died soon after birth. The causes of the babies' deaths were not brain related.

The primary cells were cultured in Dulbecco's modified Eagle's medium (DMEM)-F12 medium (Gibco, Grand Island, NY, USA) with 10% fetal bovine serum (FBS; HyClone Laboratories, Inc., Logan, UT, USA), the same medium in which UW402 and UW473 cell lines were cultured. The DAOY cell line was cultured in a-MEM (Gibco) 10% FBS and ONS-76 cell line was cultured in RPMI-1640 medium (Gibco) 10% FBS in an incubator at 37˚C and 5% CO_2. All culture

media contained penicillin at 100 units/ml and streptomycin 100 μg/ml (Gibco). The study was approved by the Ethics Research Committee of the Clinical Hospital of Ribeirão Preto and Medical School of Ribeirão Preto of the University of São Paulo under protocol number 14920/2011. All the animal procedures of the present study were conducted in agreement with the ethical principles in animal research adopted by the Brazilian College of Animal Experimentation (COBEA) and this study, under protocol number 137/2011, was also approved by the Medical School of Ribeirão Preto of the University of São Paulo, Ethics Commission of Ethics in Animal Research (CETEA).

Preparation of total RNA and microarray experiments. Total RNA was isolated from cerebellum primary cultures and medulloblastoma cell lines using RNeasy Mini kit according to the manufacturer's instructions (Qiagen, Hilden, Germany). The quantity and purity of the total RNA was determined by spectrophotometer (NanoDrop; Thermo Fisher Scientific, Waltham, MA, USA) and samples with OD 260/289 between 1.8 and 2.0 were used. In order to check the integrity of the RNA 500 ng of RNA with loading-buffer (xylene cyanol containing gelred fluorescente dye from Biotium) was loaded in a 1% miniagarose gel in Tris-Acetate-EDTA buffer. After electrophoresis, the gel was analyzed using the ImageQuant 350 transilluminator (GE Healthcare) with short-wave-length UV illumination to visualize 28S and 18S bands. The integrity of the total RNA was also evaluated by microfluidic-based electrophoresis (Agilent 2100 Bioanalyzer; Agilent Technologies, Santa Clara, CA, USA) and samples with RIN >7.0 were used for microarray experiments.

A total of 200 ng of RNA of samples and reference were reverse transcribed by the Low RNA Input linear amplification kit and then transcribed to Cy3-labelled (samples) or Cy5-labelled (reference) according to the manufacturer's instructions (Agilent Technologies). The protocols used were described in de Oliveira *et al* (39). Briefly, the reverse transcription reaction was incubated at 40˚C for 2 h and then incubated at 70˚C for 15 min to degrade the excessive RNA. Next, *in vitro* transcription was carried out using the T7 RNA polymerase and the dyes Cy3 and Cy5. This reaction was incubated at 40˚C for 2 h. After labeling and purification (Mini Spin kit; GE Healthcare), the efficiency of Cy3 and Cy5 labeling was quantified using the NanoDrop 1000 spectrophotometer (Thermo Fisher Scientific). The numerical values for the labeling efficiency were determined by the base-to-dye ratios of Cy3-dCTP and Cy5-dCTP per μg of cRNA. The values obtained were consistent with those recommended for hybridization onto cDNA microaarrays. Next, the labeled samples and reference were fragmented according to the manufacturer's instructions and the hybridization buffer added. After the arrays were loaded, the arrays were incubated at 65˚C for 17 h for hybridization.

Dye normalization was performed by the linear lowess method. For the spike in controls, the expected log ratio was plotted against the observed log ratio as a quality control check. For each lamina, the log ratio was plotted against the log processed signal to ensure that the signal strength distribution for upregulated and downregulated features were comparable.

Microarray data analysis. The raw data were obtained from a two-color Agilent platform (SurePrint G3 Human Gene Expression 8x60K Microarray kit; G4851A) using DAOY1 as a common reference. Quantile normalization was performed on the raw data after hybridization followed by normalization between arrays to obtain the gene expression levels. Expression levels for the various *HOX* genes were obtained by mapping probe names to the *HOX* genes using the NCBI GenBank. Whenever there were multiple probes present for the same *HOX* gene, the average over all probes was taken to determine the expression level for that particular gene.

All heatmaps were generated using the gplots package of Bioconductor. The identification of differentially expressed genes was performed using the Limma package in Bioconductor. A significance threshold of 0.05, along with P-values adjusted according to the Benjamini-Hochberg method, was used to determine which genes were differentially expressed. Anova contrasts were used to identify differentially expressed genes in the various comparisons shown in Fig. 1C and D. All P-values were converted to their log to the base 10 equivalents before use in Fig. 1C and D. The log fold change values used in the figures were those obtained from the Limma output.

The raw data from high-throughput microarray experiments are available on the Gene Expression Omnibus (GEO) website under accession number GSE95684.

Real-time PCR. The cDNA was directly synthesized from 1 μg total RNA from cerebellum primary cultures and medulloblastoma cell lines using the High Capacity cDNA Reverse Transcription kit (Life Technologies, Carlsbad, CA, USA) according to the manufacturer's protocol. Each 25 μl cDNA synthesis reaction solution contained 1 μg of total RNA, 1X buffer, 1X random primers, dNTP (8 mM), RNase inhibitor (2 U) and 62 U of MultiScribe Reverse Transcriptase (Life Technologies). The cDNA synthesis was carried out with 1 cycle at 25˚C for 10 min, 1 cycle at 37˚C for 120 min followed by heating to 85˚C for 5 min to terminate the reaction. Gene expression of the two HOX genes were quantified using the TaqMan Universal Master Mix as previously reported by Covas *et al* (40) and Fontes *et al* (41). Briefly, cDNA (2 μl of cDNA diluted 1:10) was applied in the real-time PCR assay with TaqMan probes (Applied Biosystems, Waltham, MA, USA) *HOXA10* (Hs00172012_m1), *HOXB4* (Hs00256884_m1) and the TaqMan Universal Master Mix according to the manufacturer's protocol. Beta actin (ACTB) gene (4310881E) was used as reference gene. Cycling was done for 2 min at 50˚C, followed by denaturation at 95˚C for 10 min. The amplification was carried out with 40 cycles of 15 sec at 95˚C and 60 sec at 60˚C. We obtained the number of amplification cycles needed for reaching the threshold fluorescence within the log-linear phase of the amplification curves after setting the appropriate baseline in each color channel of the GeneAmp® 7500 software using the manual baseline method. The relative expression level of target gene was shown as expression relative units (ERU) and was quantified according to the formula ERU = $10{,}000/2^{dCT}$ following Albesiano *et al* (42), where ΔCT = CT target sample - CT reference sample. As in the study by Albesiano, the reference gene level (in our case ACTB level) is set equal 10,000. For each sample in Fig. 2A and B, cDNA was independently

synthesized three times, and two technical replicates were carried out on each batch of independently synthesized cDNA. The same procedure was followed for the samples in Fig. 3C and E.

Gene silencing. The lentiviral particles (Santa Cruz Biotechnology, Santa Cruz, CA, USA) used contained the sequences of short hairpin for human *HOXA10* gene (shHOXA10), the green fluorescent protein (*GFP*) reporter gene and the resistance gene to the puromycin antibiotic (PUR), described as sh*HOXA10*-GFP-PUR, and the empty vector control containing only the *GFP* and *PUR* gene sequences (sh-GFP-PUR). The DAOY cell line was transduced using hexadimethrine bromide (6 μg/ml; Sigma-Aldrich, St. Louis, MO, USA) at a multiplicity of infection (MOI) of 5. After 24 h, the cells were treated with puromycin antibiotic (1 μg/ml; Sigma-Aldrich, Hamburg, Germany) for 6 days. Cell lines were identified as DAOY/sh*HOXA10*$^+$ and DAOY/control. The cell transduction efficiency was evaluated by fluorescence microscopy and flow cytometry for GFP, and gene silencing efficiency was evaluated by real-time PCR and western blot analysis.

Gene overexpression. The human *HOXB4* gene was over-expressed in UW473 the cell line by the cell transduction method. The vector used contained the sequences of human *HOXB4* gene, the *GFP* reporter gene and the resistance gene to the antibiotic puromycin, described as *HOXB4*-PUR-GFP (VB150311-10017; Cyagen Biosciences, Santa Clara, CA, USA). As a control, we used an empty vector containing only the *GFP* and *PUR* gene sequences (VB150311-10018; Cyagen Biosciences). Vectors related to the viral capsid (8.91) and viral envelope (VSV-G) were used as accessory vectors for the production of lentiviruses by transfection of the 293FT cell line using Lipofectamine™ 2000 (Invitrogen, Carlsbad, CA, USA) according to the manufacturer's protocol. The UW473 cell line was transduced with *HOXB4*-GFP-PUR and control lentiviral particles with a MOI of 2. After 24 h, the cells were treated with puromycin antibiotic (1 μg/ml; Sigma-Aldrich) for 6 days. Cell lines were identified as UW473/*HOXB4*$^+$ and UW473/control. The cell transduction efficiency was evaluated by fluorescence microscopy and flow cytometry for GFP, and HOXB4 overexpression efficiency was evaluated by real-time PCR and western blot analysis.

Western blot analysis. Total protein was extracted using RIPA buffer (Sigma-Aldrich, St. Louis, MO, USA) supplemented with protease inhibitor (Complete Mini Protease Inhibitor Cocktail; Roche Diagnostics GmbH, Mannheim, Germany) and phosphatase (PhosSTOP phosphatase inhibitor cocktail; Roche Diagnostics), and quantified using the BCA protein assay kit (Pierce, Rockford, IL, USA) according to the manufacturer's protocol. Proteins were separated by SDS-PAGE using 10% polyacrylamide gels (Mini-PROTEAN TGX; Bio-Rad Laboratories, Hercules, CA, USA), transferred from the gel to a nitrocellulose membrane (40 μm, Hybond-C extra; Amersham Biosciences, Little Chalfont, UK) and incubated in a 5% skim milk blocking solution. The following primary antibodies were used: mouse anti-human *HOXA10* (E-12) (1:250, sc-271139; Santa Cruz Biotechnology), mouse anti-human *HOXB4* (D-1) (1:500, sc-365927; Santa Cruz Biotechnology), rabbit anti-human β-actin (1:4,000, #4967; Cell Signaling Technology, Danvers, MA, USA) and rabbit anti-human *GAPDH* (14C10) (1:4,000, #2118; Cell Signaling Technology). Mouse anti-sheep IgG (1:4,000, NA931V; GE Healthcare, Aurora, OH, USA) and goat anti-mouse IgG rabbit (1:4000, #7074; Cell Signaling Technology) HRP-conjugated secondary antibodies were used. The proteins bands on the membrane were developed using ECL Western Blotting Detection Reagent Prime kit (GE Healthcare) according to the manufacturer's instructions. As mentioned by Ferguson *et al* (43) β-actin and β-tubulin proteins (both being part of the cytoskeleton of eukaryotic cells), and GAPDH enzyme (glyceraldehyde-3-phosphate dehydrogenase), are classically used as internal standards for normalization of signals in western blot analysis in order to compare differences in the expression of the target proteins among samples and eliminating variations arising from technical reasons, such as differences in amount of total load protein (43). The protocols have been previously used by various co-authors of this study, as described in Thomé *et al (*44) (β-actin) and Palma *et al (*45) who have used both these control antibodies. As in this study, in Palma *et al (*45) both control antibodies, β-tubulin and GAPDH, were used.

In vitro proliferative and migration potential assay. The proliferative potential was assessed by cell counting in a Neubauer chamber. Initially, $8x10^4$ viable cells were cultured in 75-cm^2 flask for a period of 120 h. Next, the cells were trypsinized and viable cells were counted in the Neubauer Chamber with trypan blue in quadruplicate. The proliferative potential (PP) was calculated as PP = N - No, in which N is the final number of cells and No is the initial number of cells.

Scratch assay was used to evaluate the migration potential. Cells were cultured in 6-well plates (in triplicate for each cell line), and when they reached ~95% confluence a scratch was made. The wells were photodocumented by phase contrast microscopy (Olympus IX71 and PD controller software, USA) in two different points along the scratch in each well, and identified as time 0. After 16 or 20 h, the wells were again photodocumented at the same positions using the TScratch software (software developed by Tobias Gebäck and Schulz, ETH Zurich, Switzerland). The percentage of scratch area was measured in the images of initial and final time. The migration potential was calculated as percentage of migrated area (%MA), %MA = 1- (N/No), in which N is the final area (%) and No is the initial area (%).

In vivo tumorigenic potential assay. Male nude mice weighing 20-25 g were obtained from the Central Animal House of the University of São Paulo (Ribeirão Preto, Brazil), and were housed at 23±2C with 12-h light/dark cycle. This experimental protocol was approved by the Animal Research Ethical Committee of the Medical School of Ribeirão Preto, USP (protocol number 137/2011).

For the evaluation of the tumorigenic potential, $3x10^6$ cells of medulloblastoma cell lines in 100 μl of Matrigel (Matrigel® Matrix; Corning, Inc., Corning, NY, USA) were infused subcutaneously into the backs of nude mice, which were previously anesthetized with a mixture of 2% isoflurane and

oxygen. The mice were monitored in the periods 7, 15, 30 and 60 days after cell infusion, for the detection and quantification of GFP fluorescence using the *in vivo* imaging system IVIS Lumina and Living Image software (Perkin-Elmer, Waltham, MA, USA); and for measurement of the nodular Volume using a digital caliper. The nodular volume (NV) was calculated as: NV= L x W x H x 4/3 π, where L is the length, W is the width and H is the nodule height.

Statistical analysis. The Student's t-test and the one-way ANOVA test were used to evaluate the *HOX* expression level differences, as well as migration and proliferation potential, before and after genetic modification of the MB cell lines. For these assays, statistical tests were performed using the GraphPad Prism 5 for Mac OS X. All results were expressed as mean ± standard deviation. R was used for all other statistical analyses. Tests were declared statistically significant for $P<0.05$.

Results

Higher numbers of HOX genes are significantly deregulated in DAOY and ONS-76 cell lines compared to UW473 and UW402 cell lines. In Fig. 1 we show the results of hierarchical clustering of 39 HOX genes with tumor cell lines which are not characterized (UW473 and UW402 cell lines) and primary cell cultures from the cerebellum (CP4, CP5 and CP6), and also 39 *HOX* genes with tumor cell lines which are characterized as being from the SHH subgroup (ON-S76 and DAOY cell lines) (Fig. 1A and B) (35,46,47).

In both dendograms tumor cell lines and primary cell cultures fall into two distinct groups. For the DAOY and ONS-76 cell lines this distinction is even clearer producing two distinct clusters (Fig. 1B). We observed that in DAOY and ONS-76 cell lines several *HOX* genes are expressed, while these genes are not expressed in primary cell cultures. As regards the other two cell lines, we observed a distinction between *HOX* gene profiles in UW473 and UW402 cell lines. *HOX* genes are more expressed in UW402 cell line compared with UW473 cell line (Fig. 1A).

To visualize the significantly dysregulated HOX genes we constructed the volcano plot. We observed that in the UW402 and UW473 cell lines only 6 *HOX* genes are significantly upregulated (*HOXB9*, *HOXB13*, *HOXC6*, *HOXC13*, *HOXD10* and *HOXD11*) compared with the primary cell lines from cerebellum (Fig. 1C). On the other hand, in the DAOY and ONS-76 cell lines 24 HOX genes are significantly upregulated: nine from *HOXA* group (*HOXA2*, *HOXA3*, *HOXA4*, *HOXA5*, *HOXA6*, *HOXA7*, *HOXA9*, *HOXA10* and *HOXA13*), six from *HOXB* group (*HOXB2*, *HOXB4*, *HOXB5*, *HOXB6*, *HOXB7* and *HOXB9*), six from *HOXC* group (*HOXC4*, *HOXC5*, *HOXC6*, *HOXC9*, *HOXC10* and *HOXC13*) and three from *HOXD* group (*HOXD3*, *HOXD10* and *HOXD11*) (Fig. 1D). Out of these 24 HOX genes, *HOXA3* was the most dysregulated gene, however, upregulation of this gene has not been demonstrated in medulloblastoma or other tumor from the central nervous systems (CNS). These results are summarized in Table I, which contains all log fold change values. Gene names in bold face are those mentioned above as being statistically significantly upregulated.

Table I. Comparison of fold change using microarray data set from *HOX* genes in UW402 and UW473 vs. cerebellum primary cells and DAOY and ONS-76 vs. cerebellum primary cells.

UW473 and UW402		DAOY and ONS-76	
Genes	Log fold change	Genes	Log fold change
HOXA1	-0.569958863	HOXA1	-0.597828379
HOXA2	0.095698182	**HOXA2**	2.656257452
HOXA3	2.500799762	**HOXA3**	5.535882266
HOXA4	0.803518199	**HOXA4**	3.429616377
HOXA5	1.091665053	**HOXA5**	2.184209412
HOXA6	1.611731106	**HOXA6**	2.779732951
HOXA7	1.371254281	**HOXA7**	2.825761681
HOXA9	-0.262664551	**HOXA9**	1.664946587
HOXA10	0.131334357	**HOXA10**	1.866723269
HOXA11	0.143180662	HOXA11	1.846451081
HOXA13	2.670226837	**HOXA13**	3.755042843
HOXB1	0.946528446	HOXB1	0.324546332
HOXB2	-0.182254131	**HOXB2**	3.150953293
HOXB3	2.293320983	HOXB3	1.472715878
HOXB4	0.483773574	**HOXB4**	4.027400665
HOXB5	0.726902915	**HOXB5**	4.049698398
HOXB6	2.769873572	**HOXB6**	3.992872898
HOXB7	1.744203467	**HOXB7**	2.169081951
HOXB8	0.213373435	HOXB8	2.286976211
HOXB9	3.155648057	**HOXB9**	4.359008666
HOXB13	4.43490889	HOXB13	2.78047806
HOXC4	2.657559554	**HOXC4**	4.752524627
HOXC5	0.994376614	**HOXC5**	1.697798782
HOXC6	4.164237557	**HOXC6**	3.346096371
HOXC8	1.042329918	HOXC8	1.991863755
HOXC9	2.852715702	**HOXC9**	4.663234774
HOXC10	2.095372335	**HOXC10**	2.858686398
HOXC11	-0.378263228	HOXC11	-0.496091564
HOXC12	0.317817366	HOXC12	1.876619216
HOXC13	4.232848464	**HOXC13**	3.531212456
HOXD1	0.307750142	HOXD1	1.833684289
HOXD3	0.779984978	**HOXD3**	1.743693697
HOXD4	0.924886063	HOXD4	1.133382434
HOXD8	1.49312174	HOXD8	2.089211292
HOXD9	1.620166724	HOXD9	1.288963756
HOXD10	3.44561321	**HOXD10**	4.045820474
HOXD11	2.529309801	**HOXD11**	2.805492204
HOXD12	0.064926757	HOXD12	0.579149569
HOXD13	1.71540358	HOXD13	3.112325861

From the results of these analyses, we continued the present study with focus on two genes *HOXA10* and *HOXB4*, which are significantly upregulated in DAOY and ONS-76

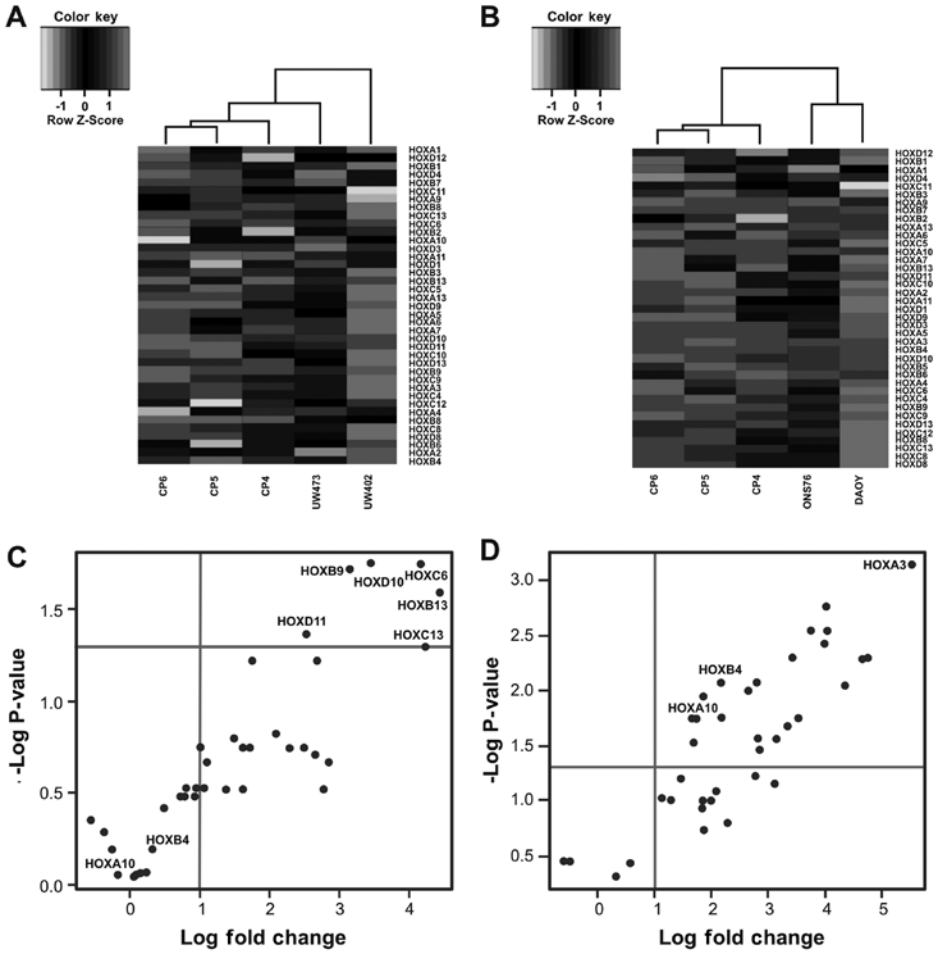

Figure 1. Total mRNA analysis identifies the *HOX* genes that are differentially expressed in UW402, UW473, DAOY and ONS-76 MB cell lines compared with three primary cell cultures from the cerebellum (CP4, CP5 and CP6). (A) A heatmap showing the separation of UW473 and UW402 cell lines and primary cells from cerebellum based on the expression pattern of all 39 HOX genes. (B) A heatmap showing the separation of DAOY and ONS-76 cell lines and primary cells from cerebellum based on the expression pattern of all 39 HOX genes. (C, D) Volcano plots with differentially expressed HOX genes. The black lines indicate genes significant at adjusted P<0.05 and fold change >1.5.

cell lines but not in UW402 and UW473. In mice MB-derived cancer stem cell (CSC), *HOXA10* has been found to be one of the top-ranking genes highly expressed in highly tumorigenic (HT)-CSCs. Also, *HOXA10* was found to have a high protein expression level in glioblastoma-derived neurospheres, and is associated with poor outcomes and treatment resistance in glioblastoma multiforme (GBM) (48). Moreover, the *HOXA10* locus was associated with expression of a stem cell related *HOX*-signature in glioblastoma and with temozolomide resistance (49). *HOXB4* was found to be expressed in medulloblastoma tissues (31) and recently, loss of *Ezh2*, an epigenetic regulator of *HOX* genes, drives aggressive medulloblastoma and was accompanied by upregulation of *HOXB4* (32).

We validated the microarray data of *HOXA10* and *HOXB4* genes and compared gene expression levels by RT-qPCR in these four MB cell lines and control cells. As seen from Fig. 2A and B, *HOXA10* and *HOXB4* are upregulated in ONS-76 and DAOY, consistent with the results from the microarray analysis. The analysis showed that *HOXA10* and *HOXB4* transcripts are not expressed in primary cerebellum cells. Previous studies by Takahashi *et al* (15) and Hutlet *et al* (16) have demonstrated the absence of *HOXA10* expression in human and mouse cerebellum tissues. These authors also showed the expression of HOX genes belonging to the 8 paralogy groups (PG1-8), which includes HOXB4, but not HOXA10. Therefore, one possible explanation for the absence of the *HOXB4* expression in our primary cerebellum culture could be due to the differences between tissues and isolated cells. In cell therapy studies differences in gene expression between tissues and isolated cells have been previously observed (40,50). In our analysis of cell lines, *HOXA10* transcripts are not expressed in two of the MB cell lines, UW402 and UW473. In the ONS-76 and DAOY cell lines, the observed expression levels of *HOXA10* are 502.4±16.07 and 1305±22.42 URE, respectively (Fig. 2A). As regards the *HOXB4* transcripts, they are expressed at low level in the UW402 and UW473 cell lines 1.05±0.16 URE and 1.072±0.33 URE, respectively. In the ONS-76 and DAOY cell lines, the expression levels of *HOXB4* transcripts are 178.4±15.85 URE and 192.5±1.97 URE, respectively (Fig. 2B).

To better understand the classification of these four MB cell lines, we examine the expression levels of 22 signature genes proposed by Northcott *et al (*6) for molecular characterization of MB subgroups (*Shh*, *Wnt*, group C and group D). As shown Fig. 2C, we observed that under our culture conditions, in the DAOY cell line two *Shh* markers (*EYA1* and *PDL*) but also the *Wnt* marker (*WIF1*) and the group C marker

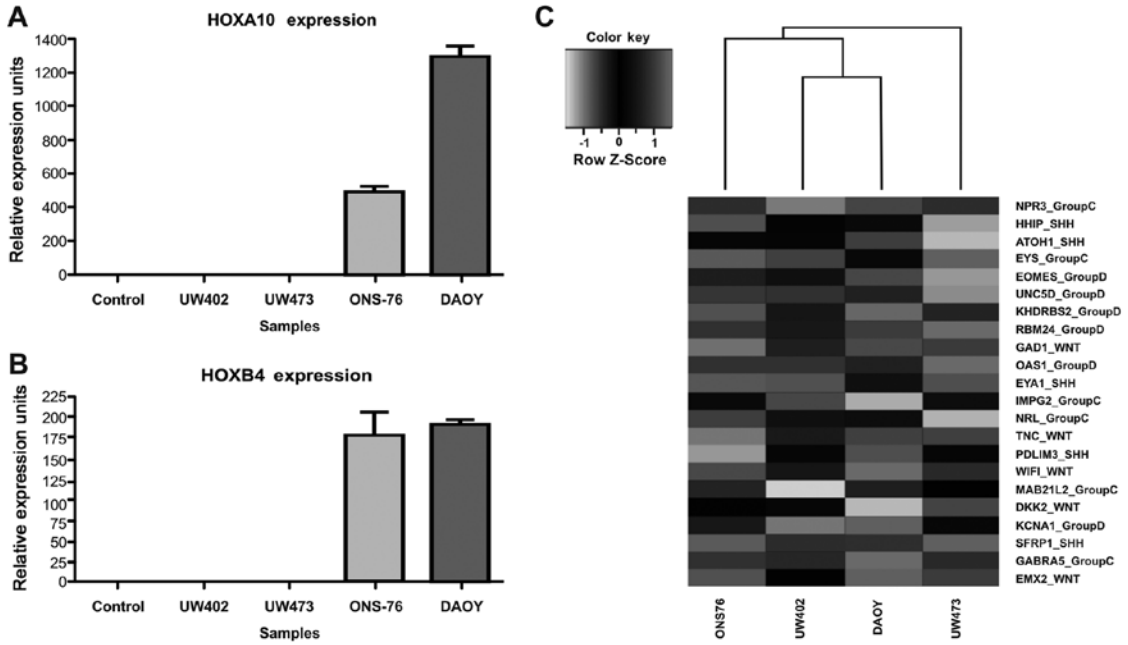

Figure 2. Quantitative validation of the microarray results by real-time PCR for *HOXA10* and *HOXB4* genes in MB cell lines and primary cells from cerebellum. (A) Quantitative RT-qPCR analysis was performed using total RNA from DAOY, ON-S76, UW402 and UW473 cell lines and primary cells from the cerebellum. The amount of *HOXA10* transcript is relative to β-actin. (B) Quantitative RT-qPCR analysis was performed using total RNA from DAOY, ON-S76, UW402 and UW473 cell lines and primary cells from the cerebellum. The amount of *HOXB4* transcript is relative to β-actin. (C) Heat Map showing the clustering between ON-S76, UW402, DAOY73 and UW473 generated by the 22 genes known from Northcott *et al* (6) to separate WNT SHH, group C and group D of medulloblastoma.

(*GABRA5*) are expressed. In the ONS-76 cell line the *Shh* marker (*HHIP*) and the group C markers (*MAB21L2*, *EYS* and *NPR3*) are expressed. On the other hand, in the UW473 cell line, genes from the four subgroups [*GAD1* (from WNT), *EYA1* [from *Shh*], *EYS* and *NPR3* (from group C)] and *OAS1* and *RBM24* (from group D) are expressed and in the UW402 cell line genes from four subgroups [*TNC* and *GAD1* (from *Wnt*), *SFRP1* (from *Shh*), *IMPG2* (from group C) and *EOMES* (from group D)] (Fig. 2C) are expressed.

Next, we investigated whether or not the *HOXA10* gene has a direct effect on the *in vivo* tumorigenic potential and on the *in vitro* proliferative and migration potential of DAOY cell line by knockdown of this transcript. We also investigated whether or not *HOXB4* transcripts have a direct effect on the *in vivo* and the *in vitro* properties in UW473 cell line after overexpression of this gene.

HOXA10 knockdown increases the migration potential but does not affect the proliferative potential of the DAOY medulloblastoma cell line. The *HOXA10* gene was silenced in the DAOY cell line by sh*HOXA10* and an empty vector was used as control. The transduction efficiency was evaluated by fluorescence microscopy and flow cytometry, which showed that >95% of DAOY/sh*HOXA10*$^+$ cells were *GFP*$^+$ (Fig. 3A). The *HOXA10* knockdown was confirmed; the *HOXA10* mRNA levels were reduced by 78% in comparison with the DAOY-control cells (268.1±16.25 vs. 59.20±2.1 URE) (P=0.0002) (Fig. 3C). The HOXA10 protein levels were also reduced in DAOY/sh*HOXA10*$^+$ cells (Fig. 3D). Analyzing the migration potential, the DAOY/sh*HOXA10*$^+$ cells displayed showed a migrated area 37±8% bigger when compared to DAOY-control cells (P=0.0046) (Fig. 4A and B). However, no difference was observed in the proliferative potential in which DAOY/sh*HOXA10*$^+$ and DAOY/control cells showed a similar amount of viable cells after 120 h of cell culture (P=0.868) (Fig. 4C). This result suggests that the low expression of *HOXA10* gene is associated with an increase in the *in vitro* migration potential; however, there is no relationship with the *in vitro* proliferative potential of the DAOY medulloblastoma cell line.

HOXB4 overexpression decreases the proliferative and migration potential of the UW473 medulloblastoma cell line. The *HOXB4* gene was overexpressed in the UW473 cell line and the transduction efficiency was evaluated by fluorescence microscopy and flow cytometry, which showed that >93% of cells were *GFP*$^+$ in UW473/*HOXB4*$^+$ and UW473-control cells (Fig. 3B). We also compared gene expression levels of *HOXB4* by qPCR in UW473-control cells and in UW473/*HOXB4*$^+$ cells. We observed that in UW473-control cells *HOXB4* mRNA is present at a very low level (1.05±0.69 URE). However, in UW493/*HOXB4*$^+$ cells the expression level of HOXB4 is 33.735±2.971 URE (P=0.0077) (Fig. 3E and F). Assessing the migration potential, the UW473/*HOXB4*$^+$ cell line showed a migrated area 32±15% smaller when compared to the UW473-control cells (P=0.033) (Fig. 5A and B). The UW473/*HOXB4*$^+$ cells line also showed a proliferative potential 34±6% lower compared to the UW473-control cells (P=0.032; Fig. 5C). These results suggest that the high expression of the *HOXB4* gene is associated with a decrease in the *in vitro* proliferative and migration potential of the UW473 medulloblastoma cell line.

HOXA10 gene silencing and HOXB4 gene overexpression do not affect the tumorigenic potential of medulloblastoma

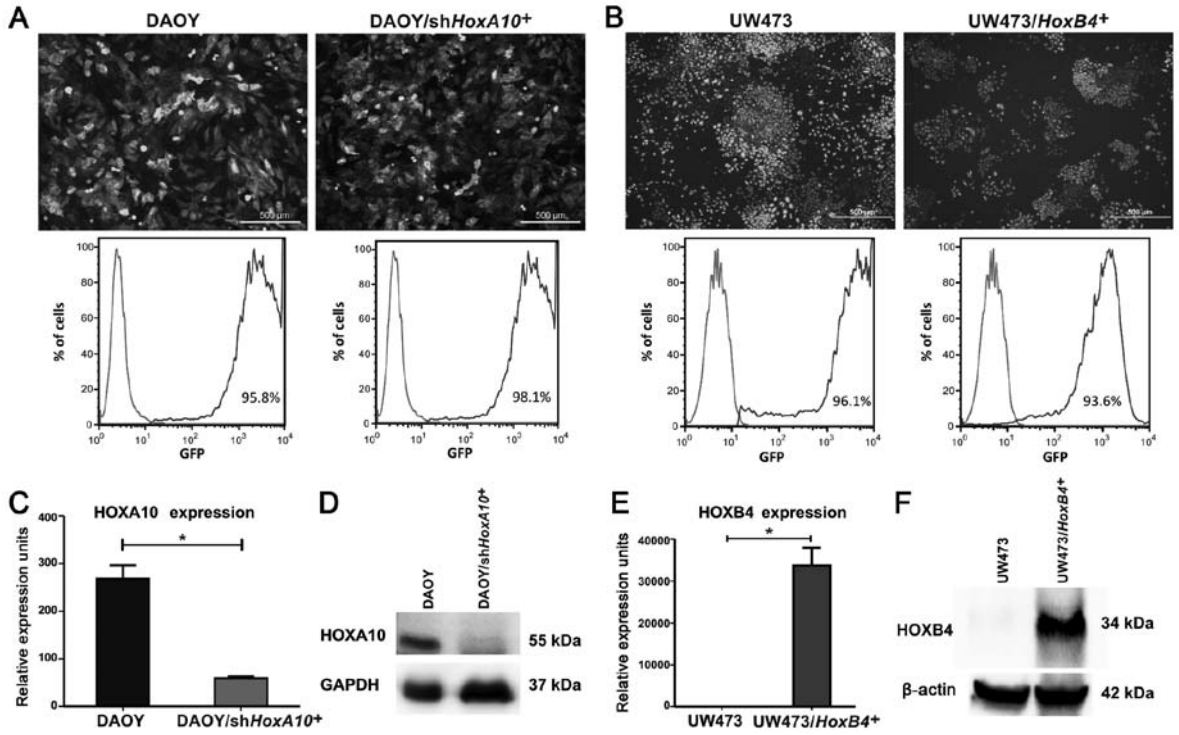

Figure 3. DAOY cells were transduced with sh*HOXA10*-GFP-PUR and UW473 cells were transduced with *HOXB4*-GFP-PUR in order to investigate the effect of *HOXA10* knockdown and *HOXB4* overexpression in these cells. Control cells were transduced with empty vectors. (A, C and D) Generation and characterization of DAOY/sh*HOXA10*$^+$ cells and DAOY-control cells (with empty vector). (B, E and F) Generation and characterization of UW473-*HOXB4*$^+$ cells and UW473-control cells (with empty vector). The transduction efficiency was evaluated by fluorescence microscopy and flow cytometry and >93% of the cells were GPF$^+$ cells. Scale bar corresponds to 500 μm. The *HOXA10* gene was silenced in DAOY/sh*HOXA10*$^+$ cells and the *HOXB4* gene was overexpressed in UW473/*HOXB4*$^+$ cells. The *HOXA10* and *HOXB4* expression levels were assessed by quantitative RT-qPCR analysis. The amount of *HOXA10* and *HOXB4* transcripts are relative to β-actin. The *HOXA10* mRNA was reduced by 78% in comparison with the control cells. The *HOXB4* mRNA was increased by 33.735±2.971 URE in comparison with control cells. Student's t-test was used with significance level of 0.05. The HOXA10 and HOXB4 proteins were assessed by western blot analysis. HOXA10 and HOXB4 proteins are present at the expected size. The HOXA10 protein level is decreased in DAOY/sh*HOXA10*$^+$ cells compared with DAOY-control cells and the HOXB4 protein level is increased in UW473/*HOXB4*$^+$ cells compared with UW473-control cells.

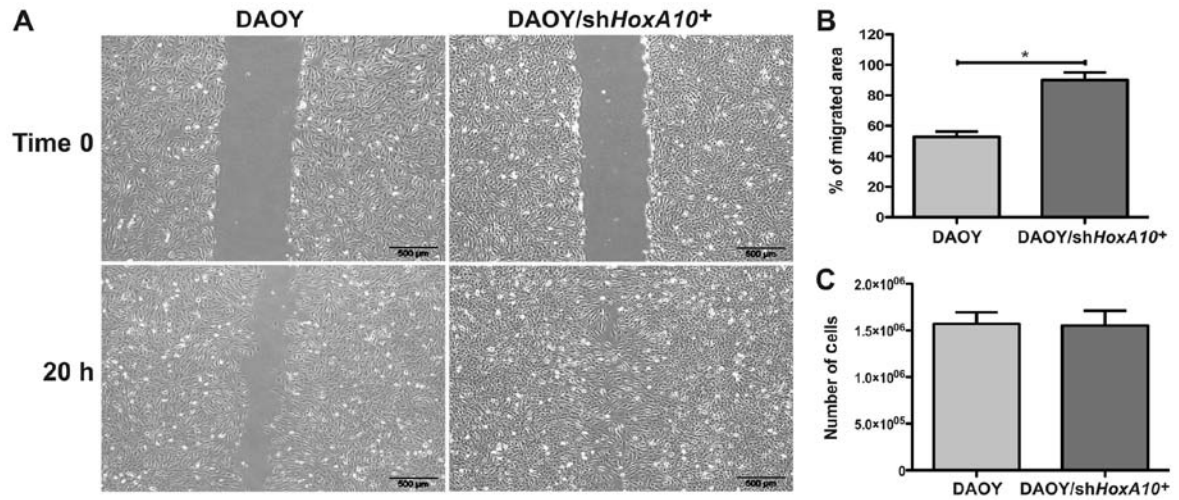

Figure 4. Effect of *HOXA10* knockdown on *in vitro* proliferative and migration potential of the DAOY cells. The DAOY/sh*HOXA10*$^+$ cells showed higher migration potential and similar proliferative potential compared to DAOY-control cells. The cell migration potential was evaluated by scratch assay (three replicates were performed) and the result was expressed as percentage of migrated area after 20 h. (A) Representative image from a scratch assay experiment of DAOY-control and DAOY/sh*HOXA10*$^+$ cell lines at time 0 and 20 h after the scratch. Contrast phase microscopy was used. (B) Quantification of the percentage of a migrated area after a period of 20 h using the Tscratch software. Results shown as mean ± standard deviation. The Student's t-test was used with 0.05 significance level (P=0.0046). (C) Proliferative potential as measured by counting the number of viable cells in the Neubauer chamber after 120 h of cell culture. Three replicates were performed.

cell lines. The effect of *HOXA10* gene inhibition and *HOXB4* gene overexpression on the tumorigenic potential of medulloblastoma cell lines was evaluated. DAOY/sh*HOXA10*$^+$, UW473/*HOXB4*$^+$, DAOY-control and UW473-control cells

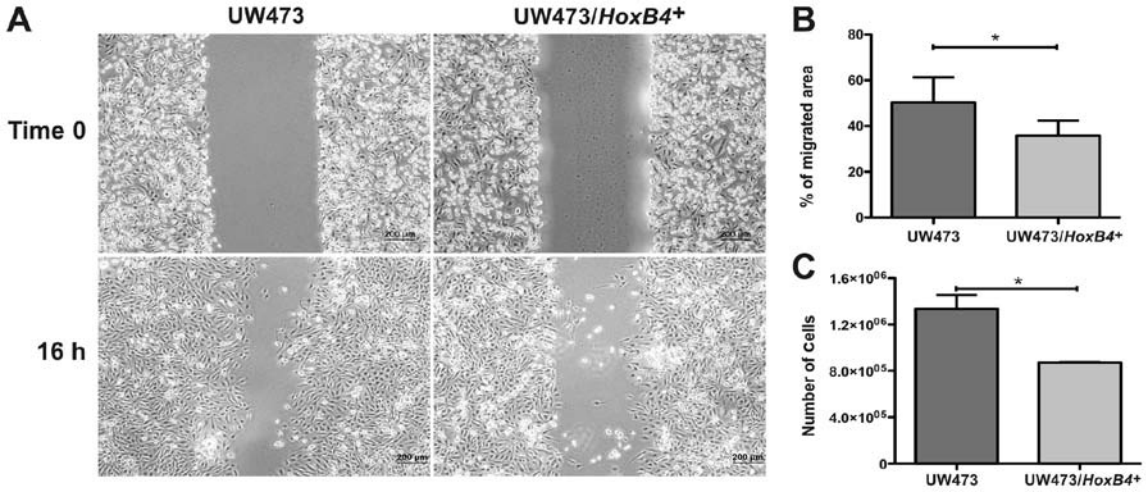

Figure 5. Effect of *HOXB4* overexpression in the *in vitro* proliferative and migration potential of the UW473 cells. The UW473/*HOXB4*$^{+}$ cells presented lower proliferative and migration potential compared to the UW473-control cells. The migration potential was evaluated by scratch assay and the result was expressed as the percentage of migrated area after 16 h. The proliferative potential was evaluated by counting viable cells in the Neubauer chamber after 120 h of cell culture. Three replicates were performed. The Student's t-test was used for statistical test with 0.05 significance level. (A) Representative image from a scratch assay experiment of UW473-control and UW473/*HOXB4*$^{+}$ cells at time 0 and 16 h after the scratch. (B) Quantification of the percentage of migrated area after a period of 16 h using the Tscratch software. Results shown as mean ± standard deviation, P=0.032. (C) Proliferative potential was measured by counting the number of viable cells in the Neubauer chamber after 120 h (P=0.033).

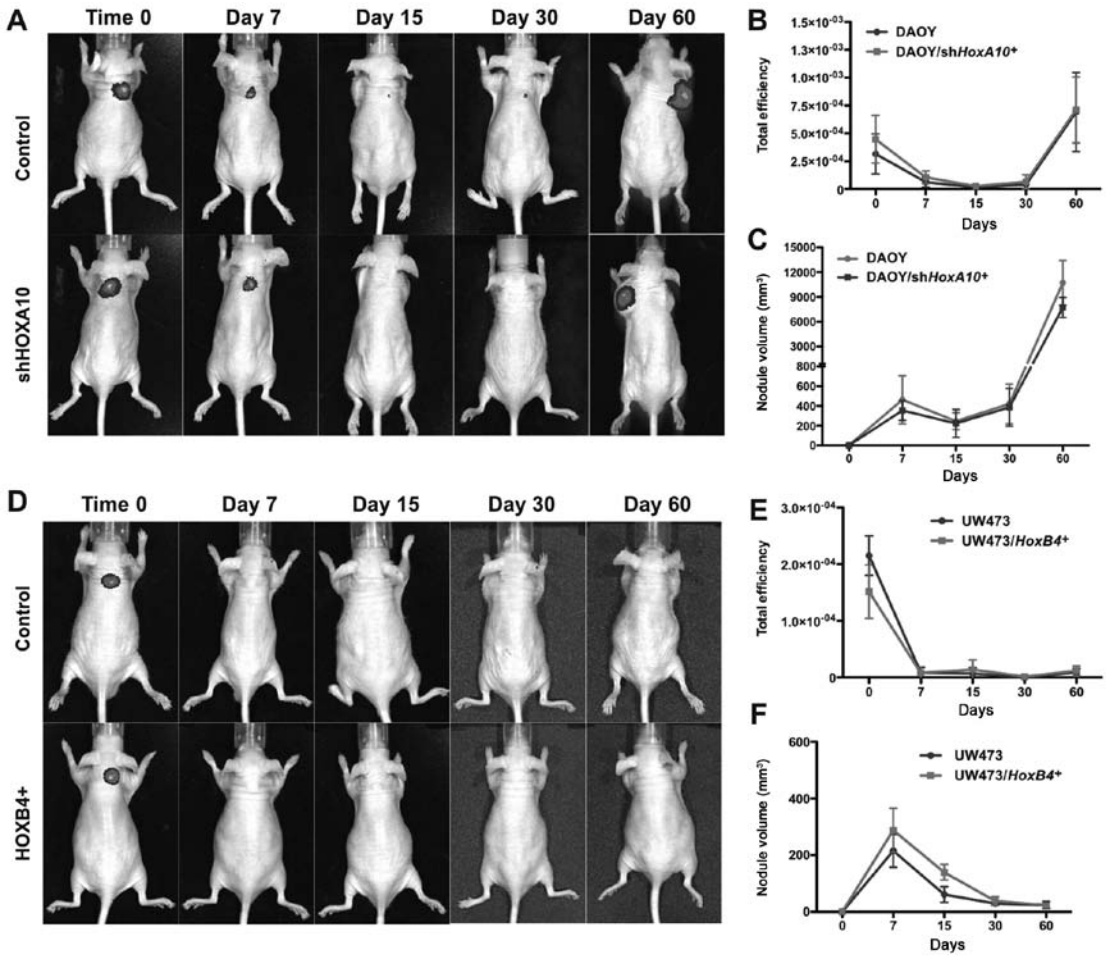

Figure 6. Effect of *HOXA10* knockdown and *HOXB4* overexpression in the *in vivo* tumorigenic potential of medulloblastoma cell lines. There was no difference in tumor volume and GFP fluorescence intensity between tumor nodules generated from the injection of DAOY-control and DAOY/sh*HOXA10*$^{+}$ cells, and there was no formation of tumor nodules from the injection of UW473-control and UW473/*HOXB4*$^{+}$ cells after 60 days of the subcutaneous cell injection in mice (n=3 in each DAOY group and n=5 in each UW473 group). The mice were monitored for a period of 7, 15, 30 and 60 days. (A and D) Representative images of the GFP fluorescence intensity emitted by GFP^{+} cells using the IVIS Lumina equipment. (B and E) Quantification of the GFP fluorescence intensity using the Living Image software. (C and F) Quantification of the nodular volume using a digital caliper. The Student's t-test was used at each time-point separately with a significance level of 0.05.

were injected subcutaneously in mice and the GFP fluorescence intensity and tumor volume were monitored for a period of 7, 15, 30 and 60 days. After 60 days, the *GFP* fluorescence intensity (Fig. 6A and B) and tumor volume (Fig. 6C) were similar in DAOY-control and DAOY/sh*HOXA10*$^{+}$ cell lines with both cell groups giving rise to tumor nodules. No formation of tumor nodules was observed in either UW473-control or UW473/*HOXA10*$^{+}$ cell lines, *GFP* fluorescence intensity (Fig. 6D and E) and tumor volume (Fig. 6F) were similar in both cell groups. These results demonstrate that the modulation of *HOXA10* and *HOXB4* gene expression did not change the tumorigenic potential of these medulloblastoma cell lines in nude mice.

Discussion

This study evaluated the differences in aberrant upregulated *HOX* gene expression among the UW402, UW473, DAOY and ONS-76 human medulloblastoma cell lines and investigated the role of two *HOX* genes (*HOXA10* and *HOXB4*) in the *in vitro* proliferative and migration potential and *in vivo* tumorigenic potential of these cell lines. Moreover, medulloblastoma is a heterogeneous disease and 22 transcripts have been used to stratify MB subgroups (6). Therefore, in order to understand these differences according to MB subtypes we compared the 22 transcript signatures in these MB-derived cell lines.

This study shows that different groups of *HOX* genes are differentially expressed according to MB-derived cell line. We identify 6 *HOX* genes (*HOXB9*, *HOXB13*, *HOXC6*, *HOXC13*, *HOXD10* and *HOXD11*) whose expression levels are significant upregulated between UW402 and UW473 cell lines and normal cerebellum primary cells; and 24 *HOX* genes (*HOXA2*, *HOXA3*, *HOXA4*, *HOXA5*, *HOXA6*, *HOXA7*, *HOXA9*, *HOXA10*, *HOXA13*, *HOXB2*, *HOXB4*, *HOXB5*, *HOXB6*, *HOXB7*, *HOXB9*, *HOXC4*, *HOXC5*, *HOXC6*, *HOXC9*, *HOXC10*, *HOXC13*, *HOXD3*, *HOXD10* and *HOXD11*) whose expression levels are significantly different between DAOY and ONS-76 cell lines and normal cerebellum primary cells.

To the best of our knowledge this is the first study that analyzes the expression pattern of all 39 *HOX* genes in MB-derived cell lines. *HOX* mRNA expression has been detected in MB tissues, Chakravadhanula *et al* (30) examined 10 MB tissues and studied the expression levels of 21 *HOX* genes. They showed that 10 *HOX* genes (*HOXC4-6*, *HOXC8-10*, *HOXD3-4*, *HOXD8* and *HOXD10*) were significantly upregulated in medulloblastoma tissues when compared to control tissues. Also, Bodey *et al* (31) observed by immunocytochemistry techniques that *HOXB3*, *HOXB4* and *HOXC6* proteins were expressed in medulloblastoma tissues. In this study some of these HOX genes are also significantly upregulated. Two of them (HOXC6 and HOXD10) are significantly upregulated in these four MB cell lines (UW473, UW402, DAOY and ONS-76) and another five (HOXC4-5, HOXC9-10 and HOXD3) were identified as significantly upregulated in DAOY and ONS-76 cells.

The noticeable change in expression levels of most HOX genes in DAOY and ONS-76 cell lines compared with UW402 and UW473 merits attention. In order to determine whether differences in *HOX* deregulation are related to MB subtype we used the 22-transcript predictor in these 4 MB cell lines. We observed that UW473 and UW402 cell lines express genes from all four MB groups, and DAOY and ONS-76 previously classified as SHH subtype (38) also express genes from the other MB subtypes. DAOY expresses SHH, WNT and group C markers and ONS-76 expresses SHH and group C markers. These results suggest that under our cell culture conditions these cell lines cannot be classified as belonging to a unique molecular subtype and therefore the interesting differences in *HOX* pattern expression among these four MB cell lines cannot be directly associated with MB subtype. A similar effect has been observed in the D238-MB cell line, which has been classified as group 4 or group 3 (51,52).

Among the *HOX* genes significantly overexpressed in DAOY and ONS-76 cell lines compared to the UW402 and UW473 cell lines we selected HOXA10 and HOXB4 as mentioned earlier. In mouse medulloblastoma (MB)-derived cancer stem cell (CSC) the role of *miR-135a*, which binds to *HOXA10* 3'UTR in other cancers, was investigated (53,54). Hemmesi *et al* (54) showed that induced overexpression of *miR-135a* in mouse MB-derived CSC was responsible for a significant decrease in the expression of *HOXA10* at mRNA level, but not at the protein level. Moreover, considering that *miR-135a* restoration inhibits tumor progression in CSC-derived MBs with no change in *HOXA10* protein level, which suggests that in MB-CSCs *HOXA10* can contribute to the malignant properties of MB cells depending on genetic background. *HOXA10* is also one of the *HOX* genes, which shows a markedly higher expression in glioblastoma-derived neurospheres and was associated with worse outcome in patients assigned to TMZ/RT-TMZ therapy (48). From our initial analysis which showed that *HOXA10* is differentially overexpressed in DAOY and ONS-76 cell lines but not in UW402 and UW473 cell lines, we decided to investigate whether knockdown of *HOXA10* in DAOY cell line will result in changes *in vitro* migration and proliferation potential changes and *in vivo* tumor growth. We observe that knockdown of *HOXA10* does in fact lead to an increase in the *in vitro* migration potential of the DAOY medulloblastoma cell line, however, there was no relationship between the *HOXA10* expression level and the *in vitro* proliferative and the *in vivo* tumorigenic potential of that cell line. Altogether, although the exact mechanism that accounts for these effects in MB is unknown, these data might indicate that *HOXA10* could contain different epigenetic regulators and has a role in several physiological processes.

Regarding the *HOXB4* gene, we investigated whether or not overexpression of *HOXB4* in the UW473 cell line promotes proliferation, migration and *in vivo* MB tumorigenesis. In the present study, we showed that the *HOXB4* expression level is associated with a decrease in the *in vitro* proliferative and migration potential of the UW473/*HOXB4*$^{+}$ cell line, however, it did not influence the *in vivo* tumorigenic potential of that cell line. It was previously known that *HOXB4* is expressed in MB tissues (31) but the effect of this gene in medulloblastogenesis was not investigated. A recent study by Vo *et al* (32) measured RNA levels of *HOXB4* gene in MB cells after gene-editing systems to induce loss-of-function mutation in *Ezh2*. In these *Ezh2*-mutated cells, *HOXB4* was expressed more highly and the tumor became more aggressive. *Ezh2* is an epigenetic regulator of *HOX* expression as a member of

polycomb-repressive complex 2 (PRC2) together with EED, SUZ12 and other accessory proteins. Altogether, these results suggest that in UW473/*HOXB4*$^{+}$ cells additional changes at the genetic or epigenetic levels are required to inactivate essential genes necessary for normal cellular development and function and to induce tumorigenesis.

To conclude, the present study was motivated by an earlier study of the importance of MLL2 in MB and the observation that MLL2 is an epigenetic regulator of the HOX gene. From the results of the microarray analysis presented (which were validated by RT-qPCR), we selected two HOX genes for functional analysis *in vitro* and in a mouse model. The *in vitro* analysis showed that these genes could be involved in migration and proliferative potential. The *in vivo* study with mice was not conclusive, which may be due to a variety of different causes. Other members of the HOX gene family could be involved. Another possibility is that MLL2 deletions have an effect on MB, but via other genes for example the MB oncogene named OTX2 or β-catenin known to regulate Wnt pathways, and which is implicated in one of the medulloblastoma subtype. Studies similar to the one we have undertaken should be extended to other genes and could help identify potential drug targets.

Acknowledgements

We thank the Conselho Nacional de Desenvolvimento Científico e Tecnológico (CNPq) (Process no. 310619/2012-2) and Fundação de Amparo à Pesquisa do Estado de São Paulo (FAPESP) (Process nos. 2011/20829-4 and 2011/18664-7) for the financial support for the present study. We also thank Sandra Navarro Bresciani of the Regional Blood Center of Ribeirão Preto-FMRP-USP, Brazil for help with the figures.

References

1. Gilbertson RJ and Ellison DW: The origins of medulloblastoma subtypes. Annu Rev Pathol 3: 341-365, 2008.
2. Louis DN, Ohgaki H, Wiestler OD, Cavenee WK, Burger PC, Jouvet A, Scheithauer BW and Kleihues P: The 2007 WHO classification of tumours of the central nervous system. Acta Neuropathol 114: 97-109, 2007.
3. Garrè ML, Cama A, Bagnasco F, Morana G, Giangaspero F, Brisigotti M, Gambini C, Forni M, Rossi A, Haupt R, *et al*: Medulloblastoma variants: Age-dependent occurrence and relation to Gorlin syndrome - a new clinical perspective. Clin Cancer Res 15: 2463-2471, 2009.
4. Ramaswamy V, Remke M, Bouffet E, Bailey S, Clifford SC, Doz F, Kool M, Dufour C, Vassal G, Milde T, *et al*: Risk stratification of childhood medulloblastoma in the molecular era: The current consensus. Acta Neuropathol 131: 821-831, 2016.
5. Northcott PA, Dubuc AM, Pfister S and Taylor MD: Molecular subgroups of medulloblastoma. Expert Rev Neurother 12: 871-884, 2012.
6. Northcott PA, Shih DJ, Remke M, Cho YJ, Kool M, Hawkins C, Eberhart CG, Dubuc A, Guettouche T, Cardentey Y, *et al*: Rapid, reliable, and reproducible molecular sub-grouping of clinical medulloblastoma samples. Acta Neuropathol 123: 615-626, 2012.
7. Gibson P, Tong Y, Robinson G, Thompson MC, Currle DS, Eden C, Kranenburg TA, Hogg T, Poppleton H, Martin J, *et al*: Subtypes of medulloblastoma have distinct developmental origins. Nature 468: 1095-1099, 2010.
8. Coluccia D, Figuereido C, Isik S, Smith C and Rutka JT: Medulloblastoma: Tumor biology and relevance to treatment and prognosis paradigm. Curr Neurol Neurosci Rep 16: 43, 2016.
9. Khatua S: Evolving molecular era of childhood medulloblastoma: Time to revisit therapy. Future Oncol 12: 107-117, 2016.
10. Parsons DW, Li M, Zhang X, Jones S, Leary RJ, Lin JC, Boca SM, Carter H, Samayoa J, Bettegowda C, *et al*: The genetic landscape of the childhood cancer medulloblastoma. Science 331: 435-439, 2011.
11. Roy DM, Walsh LA and Chan TA: Driver mutations of cancer epigenomes. Protein Cell 5: 265-296, 2014.
12. Schuettengruber B, Martinez AM, Iovino N and Cavalli G: Trithorax group proteins: Switching genes on and keeping them active. Nat Rev Mol Cell Biol 12: 799-814, 2011.
13. Wang VY and Zoghbi HY: Genetic regulation of cerebellar development. Nat Rev Neurosci 2: 484-491, 2001.
14. Ruddle FH: The role of Hox and Dlx gene cluster in evolution and development. In: Inborn Errors of Development. Epstein CJ, Erickson RP and Wynshaw-Boris A (eds). Oxford University Press, New York, pp653-658, 2008.
15. Takahashi Y, Hamada J, Murakawa K, Takada M, Tada M, Nogami I, Hayashi N, Nakamori S, Monden M, Miyamoto M, *et al*: Expression profiles of 39 HOX genes in normal human adult organs and anaplastic thyroid cancer cell lines by quantitative real-time RT-PCR system. Exp Cell Res 293: 144-153, 2004.
16. Hutlet B, Theys N, Coste C, Ahn MT, Doshishti-Agolli K, Lizen B and Gofflot F: Systematic expression analysis of Hox genes at adulthood reveals novel patterns in the central nervous system. Brain Struct Funct 221: 1223-1243, 2016.
17. Mallo M and Alonso CR: The regulation of Hox gene expression during animal development. Development 140: 3951-3963, 2013.
18. Shah N and Sukumar S: The Hox genes and their roles in oncogenesis. Nat Rev Cancer 10: 361-371, 2010.
19. Quinonez SC and Innis JW: Human HOX gene disorders. Mol Genet Metab 111: 4-15, 2014.
20. Wu X, Chen H, Parker B, Rubin E, Zhu T, Lee JS, Argani P and Sukumar S: HOXB7, a homeodomain protein, is overexpressed in breast cancer and confers epithelial-mesenchymal transition. Cancer Res 66: 9527-9534, 2006.
21. Liao WT, Jiang D, Yuan J, Cui YM, Shi XW, Chen CM, Bian XW, Deng YJ and Ding YQ: HOXB7 as a prognostic factor and mediator of colorectal cancer progression. Clin Cancer Res 17: 3569-3578, 2011.
22. Wang Y, Dang Y, Liu J and Ouyang X: The function of homeobox genes and lncRNAs in cancer. Oncol Lett 12: 1635-1641, 2016.
23. Rodrigues MF, Esteves CM, Xavier FC and Nunes FD: Methylation status of homeobox genes in common human cancers. Genomics 108: 185-193, 2016.
24. Costa BM, Smith JS, Chen Y, Chen J, Phillips HS, Aldape KD, Zardo G, Nigro J, James CD, Fridlyand J, *et al*: Reversing HOXA9 oncogene activation by PI3K inhibition: Epigenetic mechanism and prognostic significance in human glioblastoma. Cancer Res 70: 453-462, 2010.
25. Tabuse M, Ohta S, Ohashi Y, Fukaya R, Misawa A, Yoshida K, Kawase T, Saya H, Thirant C, Chneiweiss H, *et al*: Functional analysis of HOXD9 in human gliomas and glioma cancer stem cells. Mol Cancer 10: 60, 2011.
26. Se YB, Kim SH, Kim JY, Kim JE, Dho YS, Kim JW, Kim YH, Woo HG, Kim SH, Kang SH, *et al*: Underexpression of HOXA11 is associated with treatment resistance and poor prognosis in glioblastoma. Cancer Res Treat 49: 387-398, 2017.
27. Munthe S, Sørensen MD, Thomassen M, Burton M, Kruse TA, Lathia JD, Poulsen FR and Kristensen BW: Migrating glioma cells express stem cell markers and give rise to new tumors upon xenografting. J Neurooncol 130: 53-62, 2016.
28. Manohar CF, Salwen HR, Furtado MR and Cohn SL: Up-regulation of HOXC6, HOXD1, and HOXD8 homeobox gene expression in human neuroblastoma cells following chemical induction of differentiation. Tumour Biol 17: 34-47, 1996.
29. Zhang X, Hamada J, Nishimoto A, Takahashi Y, Murai T, Tada M and Moriuchi T: HOXC6 and HOXC11 increase transcription of S100beta gene in BrdU-induced in vitro differentiation of GOTO neuroblastoma cells into Schwannian cells. J Cell Mol Med 11: 299-306, 2007.
30. Chakravadhanula M, Ozols VV, Hampton CN, Zhou L, Catchpoole D and Bhardwaj RD: Expression of the HOX genes and HOTAIR in atypical teratoid rhabdoid tumors and other pediatric brain tumors. Cancer Genet 207: 425-428, 2014.
31. Bodey B, Bodey B Jr, Siegel SE and Kaiser HE: Immunocytochemical detection of the homeobox B3, B4, and C6 gene products in childhood medulloblastomas/primitive neuroectodermal tumors. Anticancer Res 20: 1769-1780, 2000.
32. Vo BT, Li C, Morgan MA, Theurillat I, Finkelstein D, Wright S, Hyle J, Smith SMC, Fan Y, Wang YD, *et al*: Inactivation of Ezh2 upregulates Gfi1 and drives aggressive Myc-driven group 3 medulloblastoma. Cell Rep 18: 2907-2917, 2017.

33. Margueron R and Reinberg D: The Polycomb complex PRC2 and its mark in life. Nature 469: 343-349, 2011.
34. Hanahan D and Weinberg RA: Hallmarks of cancer: The next generation. Cell 144: 646-674, 2011.
35. Castro-Gamero AM, Borges KS, Lira RC, Andrade AF, Fedatto PF, Cruzeiro GA, Silva RB, Fontes AM, Valera ET, Bobola M, *et al*: Chromosomal heterogeneity and instability characterize pediatric medulloblastoma cell lines and affect neoplastic phenotype. Cytotechnology 65: 871-885, 2013.
36. Jacobsen PF, Jenkyn DJ and Papadimitriou JM: Establishment of a human medulloblastoma cell line and its heterotransplantation into nude mice. J Neuropathol Exp Neurol 44: 472-485, 1985.
37. Yamada M, Shimizu K, Tamura K, Okamoto Y, Matsui Y, Moriuchi S, Park K, Mabuchi E, Yamamoto K, Hayakawa T, *et al*: Establishment and biological characterization of human medulloblastoma cell lines. No To Shinkei 41: 695-702, 1989 (In Japanese).
38. Ivanov DP, Coyle B, Walker DA and Grabowska AM: In vitro models of medulloblastoma: Choosing the right tool for the job. J Biotechnol 236: 10-25, 2016.
39. de Oliveira GP, Alves CJ and Chadi G: Early gene expression changes in spinal cord from SOD1^{G93A} Amyotrophic Lateral Sclerosis animal model. Front Cell Neurosci 7: 216, 2013.
40. Covas DT, Panepucci RA, Fontes AM, Silva WA Jr, Orellana MD, Freitas MC, Neder L, Santos AR, Peres LC, Jamur MC, *et al*: Multipotent mesenchymal stromal cells obtained from diverse human tissues share functional properties and gene-expression profile with CD146^{+} perivascular cells and fibroblasts. Exp Hematol 36: 642-654, 2008.
41. Fontes AM, Melo FU, Greene LJ, Faça VM, Lin Y, Gerson SL and Covas DT: Production of human factor VIII-FL in 293T cells using the bicistronic MGMT(P140K)-retroviral vector. Genet Mol Res 11: 775-789, 2012.
42. Albesiano E, Messmer BT, Damle RN, Allen SL, Rai KR and Chiorazzi N: Activation-induced cytidine deaminase in chronic lymphocytic leukemia B cells: Expression as multiple forms in a dynamic, variably sized fraction of the clone. Blood 102: 3333-3339, 2003.
43. Ferguson RE, Carroll HP, Harris A, Maher ER, Selby PJ and Banks RE: Housekeeping proteins: A preliminary study illustrating some limitations as useful references in protein expression studies. Proteomics 5: 566-571, 2005.
44. Thomé CH, dos Santos GA, Ferreira GA, Scheucher PS, Izumi C, Leopoldino AM, Simão AM, Ciancaglini P, de Oliveira KT, Chin A, *et al*: Linker for activation of T-cell family member2 (LAT2) a lipid raft adaptor protein for AKT signaling, is an early mediator of alkylphospholipid anti-leukemic activity. Mol Cell Proteomics 11: 1898-1912, 2012.
45. Palma CS, Grassi ML, Thomé CH, Ferreira GA, Albuquerque D, Pinto MT, Ferreira Melo FU, Kashima S, Covas DT, Pitteri SJ, *et al*: Proteomic analysis of epithelial to mesenchymal transition (EMT) reveals cross-talk between SNAIL and HDAC1 proteins in breast cancer cells. Mol Cell Proteomics 15: 906-917, 2016.
46. Triscott J, Lee C, Foster C, Manoranjan B, Pambid MR, Berns R, Fotovati A, Venugopal C, O'Halloran K, Narendran A, *et al*: Personalizing the treatment of pediatric medulloblastoma: Polo-like kinase 1 as a molecular target in high-risk children. Cancer Res 73: 6734-6744, 2013.
47. Bobola MS, Silber JR, Ellenbogen RG, Geyer JR, Blank A and Goff RD: O^{6}-methylguanine-DNA methyltransferase, O^{6}-benzylguanine, and resistance to clinical alkylators in pediatric primary brain tumor cell lines. Clin Cancer Res 11: 2747-2755, 2005.
48. Murat A, Migliavacca E, Gorlia T, Lambiv WL, Shay T, Hamou MF, de Tribolet N, Regli L, Wick W, Kouwenhoven MC, *et al*: Stem cell-related 'self-renewal' signature and high epidermal growth factor receptor expression associated with resistance to concomitant chemoradiotherapy in glioblastoma. J Clin Oncol 26: 3015-3024, 2008.
49. Kurscheid S, Bady P, Sciuscio D, Samarzija I, Shay T, Vassallo I, Criekinge WV, Daniel RT, van den Bent MJ, Marosi C, *et al*: Chromosome 7 gain and DNA hypermethylation at the HOXA10 locus are associated with expression of a stem cell related HOX-signature in glioblastoma. Genome Biol 16: 16, 2015.
50. Perkins EJ, Bao W, Guan X, Ang CY, Wolfinger RD, Chu TM, Meyer SA and Inouye LS: Comparison of transcriptional responses in liver tissue and primary hepatocyte cell cultures after exposure to hexahydro-1,3,5-trinitro-1,3,5-triazine. BMC Bioinformatics 7 (Suppl 4): S22, 2006.
51. Snuderl M, Batista A, Kirkpatrick ND, Ruiz de Almodovar C, Riedemann L, Walsh EC, Anolik R, Huang Y, Martin JD, Kamoun W, *et al*: Targeting placental growth factor/neuropilin 1 pathway inhibits growth and spread of medulloblastoma. Cell 152: 1065-1076, 2013.
52. Sengupta S, Weeraratne SD, Sun H, Phallen J, Rallapalli SK, Teider N, Kosaras B, Amani V, Pierre-Francois J, Tang Y, *et al*: α5-GABAA receptors negatively regulate MYC-amplified medulloblastoma growth. Acta Neuropathol 127: 593-603, 2014.
53. Tang W, Jiang Y, Mu X, Xu L, Cheng W and Wang X: MiR-135a functions as a tumor suppressor in epithelial ovarian cancer and regulates HOXA10 expression. Cell Signal 26: 1420-1426, 2014.
54. Hemmesi K, Squadrito ML, Mestdagh P, Conti V, Cominelli M, Piras IS, Sergi LS, Piccinin S, Maestro R, Poliani PL, *et al*: *miR-135a* inhibits cancer stem cell-driven medulloblastoma development by directly repressing *Arhgef6* expression. Stem Cells 33: 1377-1389, 2015.